JOURNAL OF MATERIALS SCIENCE **40** (2005) 27–36

Defect annihilations in carbon nanotubes under thermo-mechanical loading

C. SHET, N. CHANDRA*, S. NAMILAE
Department of Mechanical Engineering, FAMU-FSU College of Engineering, Florida State University, Tallahassee, FL 32310, USA
E-mail: Chandra@eng.fsu.edu

Topological defects can be formed in carbon nanotubes (CNTs) either during processing or during subsequent thermo-mechanical loading. When multiple defects are formed, the defects interact with each other depending upon the distance of separation between them. Earlier studies have shown that under mechanical loading, such interacting defects coalesce to form a larger defect, ultimately leading to complete failure. While defect coalescence is possible, it has also been observed that some defects may disappear (anneal) under certain thermo-mechanical conditions. In this molecular dynamics (MD) based simulation studies, we show that two 5-7-7-5 type defects (Stone-Wales) in close proximity when subjected to either pure mechanical loading (tensile strain of 10%) or pure thermal loading (temperature up to 3000 K) remain stable. On the other hand, the defects annihilate completely under a combination of both thermal (2800 K) and mechanical loading (under 5%) applied concurrently. It is hypothesized that vibrational oscillations due to thermal effects combined with atomic separation induced due to mechanical load together can cause the defects to annihilate while either of them acting alone cannot do so.

1. Introduction

The exceptional mechanical properties of carbon nanotubes (CNTs) and their potential use in structural components and devices have stimulated great interest and extensive research, ever since their discovery by Iijima [1] in 1991. However, the structural applications of CNTs in the form of reinforcements in composites depend on the elastic stiffness and strength in the embedded state. Experimental observations have revealed that topological defects such as 5-7-7-5 Stone-Wales defects are commonly present in nanotubes [2]. Strength and stiffness of CNTs are considerably affected by the presence of these defects [2, 3]; with similar effects due to vacancies, impurities or dopants and other geometrical irregularities. Studies have shown that defects in CNTs may not only affect the mechanical properties, but also electronic, magnetic and hybridization characteristics and hence need to be understood thoroughly [4–6]. The transitions in the Y-junction contemplated in CNT based molecular electronics is achieved through the incorporation of many topological defects either by design or otherwise [7]. Similarly, transition of nanotubes from one diameter to another can be achieved by locating a few of these defects strategically in the transition region. Also, when nanotubes are used as fibers in nanocomposites interfacial bonding may preferably occur in these defected regions driven by energetics.

During manufacture of CNTs, both in single and multi-walled tubes defects are formed whenever the formation conditions deviate from that of a narrow ideal range. When CNTs are subjected to uniaxial tensile loading, a 5-7-7-5 defect is formed since it releases excessive strain energy by the rotation of a C─C bond [8]. Defects are also formed in both graphene sheets and CNTs, when the applied tensile strain is in the range of 5 to 6% [9]. Because of the unique planar hexagonal mesh-like structure of the CNTs, topological defects can alter the deformation response and hence the elastic properties. In addition, these defects can also potentially initiate irreversible mechanical response [10]. Further, the topological defects also locally alter the ovality of the tubes causing nonlinear effects. These sites act as nucleation centers for the formation of dislocations in the originally ideal graphite network, and they engender the onset of plastic deformation in CNTs [11]. In the simulation of CNT under uniaxial tension. Zhou and Shi [12] have shown that multiple defects are formed prior to failure. They have also observed that near the defected region some carbon atoms having broken from its immediate neighbor move closer to second nearest neighbor and form a new carbon-carbon bond.

When topological defects of the type 5-7-7-5 are formed, the defect formation is associated with a specific quantity of energy. The defect formation energy for a 5-7-7-5 defect in a graphene sheet by direct exchange

* Author to whom all correspondence should be addressed.

method, calculated as the difference in energy between defected and perfect sheet is estimated to be 10.4 eV [13]. Defect formation energy for nanotubes depends on the geometry of the nanotube i.e., diameter and chirality of CNTs [14, 15]. The energy barrier for a defect to form is the extra energy needed to overcome a given state resulting in the rotation of a bond by 90°. This barrier energy not only depends on its geometric form such as diameter and chirality. but also on its thermomechanical state such as the thermal fluctuation and tensile strain. The barrier energy in case of a (6,6) tube is 4.0 eV and that for graphene sheet is 4.5 eV [15].

In both graphene sheets and CNTs carbon atoms are arranged in a hexagonal honeycomb pattern with sp^2 covalent bonds between the connected atoms. In the hexagonal arrangement, the carbon atoms are energetically in stable configurations. Presence of any defect will lead to energetically unstable condition. Under thermomechanical conditions. CNTs with defects heal by a reconstruction process. A few atoms near the defect realign or bond to next nearest neighbors so that a near stable configuration is attained. It has been observed by Ajayan *et al*. [16] that when a vacancy is created by removal of a carbon atom, there will be a set of three two-coordinate carbon atoms with dangling bonds. An immediate reconstruction mechanism results, when two of the three dangling bonds join together to form a pentagon. This makes the tube shrink by a small amount and change the ovality of the tube. Due to shrinking of the tube the third dangling atom moves close enough to join to the opposite pentagon (which has been created by joining of two dangling bonds) to reach metastable condition where one of the carbon atom is bonded with sp^3. Kosaka *et al*. [17] in their experimental study, measured electron spin resonance (ESR) on annealed arc-grown nanotubes (annealed at 2800°C prior to ESR measurements) and non-annealed nanotubes. The authors state that differences seen in the ESR spectra of annealed and non-annealed nanotubes indicate that some kind of defects are initially present in the tube which are then removed by annealing, however the heat treatment may not heal large defects [18]. Ajayan *et al*. [16] have shown that under controlled electron irradiation conditions, a nanotube of initial diameter of 1.4 nm shrunk to 0.4 nm. Under irradiation process, atoms are removed from the surface leaving an unstable surface structure, tending the tube to shrink by atomic rearrangements.

From the above, it can be understood that a reconstruction process takes place in a CNT with defects, where thermal and mechanical loadings play key roles in the reconstruction process. In this paper we study the reconstruction process on a group of defects in a CNT, under the effect of thermo-mechanical loading. Here, we study the annihilation process for a group of defects subjected to a combination of thermal and mechanical (tensile) loading on CNTs.

In this work, we have used molecular dynamics simulations based on Tersoff-Brenner bond-order potential, which is known to represent C–C interactions accurately. Our primary interest is to study what happens to a group of defects under the action of thermal, mechanical and combined thermo-mechanical loadings. It has been shown that the energetics of atom play a key role in defect annihilation. In a CNT with defects, the atoms forming core of the defects will have higher energy level tending them to be energetically unstable. We try to explain the mechanism of atoms jumping the energy barrier in order to reach an energetically stable configuration resulting in defect annihilation. It is observed that the defect produces stress and strain concentration effects near the defected region due to changes in the geometric configuration and concomitant force fields [4, 19]. In this work, we adopt local stress measures to examine the stress concentration effect before the defect annihilation and how the stress field varies after defect annihilation.

2. Atomic level stress

Stress is a measure defined to quantify the internal resistance of material to counter external disturbances. Stress in a simplified sense can be construed as force over an infinitesimal area as the area tends to zero in the limiting process. When we define stress at a point, in the sense of continuum mechanics we implicitly assume that a homogenous state of stress exists within the appropriately chosen infinitesimal volume surrounding that point. Here we adopt the concept of local stress advanced by Lutsko [20] and extended by Cormier *et al*. [21] to measure stress around the defected region. Lutsko stress assumes that the stress state is homogenous in the averaging volume and is based on the local stress tensor of statistical mechanics. The forces between atoms are determined by relative empirical bond order (REBO) hydrocarbon potential given by Brenner. This potential describes various properties of chemical bonding in carbon such as bond angles, lengths and conjugation. Lutsko stress σ_{ij}^{L} can be expressed as:

$$\sigma_{ij}^{L} = \frac{1}{\Omega^{Avg}} \sum_{\alpha=1,n} \left(\frac{1}{2} m^{\alpha} v_i^{\alpha} v_j^{\alpha} + \sum_{\beta=1,n} r_{\alpha\beta}^{j} f_{\alpha\beta}^{i} l_{\alpha\beta} \right) \quad (1)$$

here i, j denote the indices in Cartesian coordinate system 1, 2 and 3, while α and β are the atomic indices. $l_{\alpha\beta}$ denotes the fraction of the length of α-β bond lying inside the averaging volume Ω^{Avg}. The averaging volume can be a small part of the total volume possibly containing defects. m^{α} and v^{α} denote the mass and velocity of atom α. $r_{\alpha\beta}$ is the distance between atoms α and β and $f_{\alpha\beta}^{i} = \frac{r_{\alpha\beta}^{j}}{|r_{\alpha\beta}|} \frac{dV}{dr_{\alpha\beta}}$, where V is the pair potential and the term $\frac{dV}{dr_{\alpha\beta}}$ is the scalar of force exerted on atom α by atom β.

Extending the definition of stress to one atomic volume proposed by Basinski, Deusberry and Taylor [22] to define atomic stress (also called BDT stress) σ_{ij}^{α} for atom α can be expressed as:

$$\sigma_{ij}^{\alpha} = \frac{1}{\Omega^{\alpha}} \sum_{\alpha=1,n} \left(\frac{1}{2} m^{\alpha} v_i^{\alpha} v_j^{\alpha} + \sum_{\beta=1,n} r_{\alpha\beta}^{j} f_{\alpha\beta}^{i} \right) \quad (2)$$

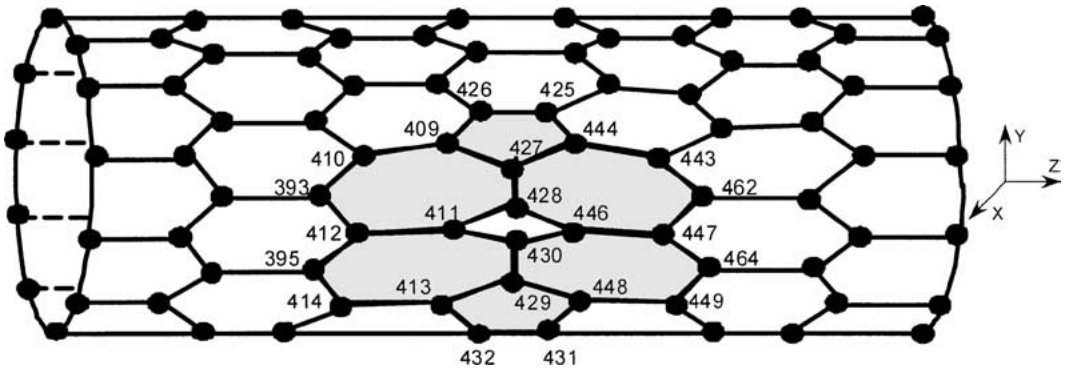

Figure 1 Two 5-7-7-5 defects placed along the circumference of the tube. The numbers indicate the atom numbers forming the defects.

Theoretically, the above definitions are valid only for homogenous systems, though BDT stress gives a fair indication of the nature of stresses in systems with defects and has been used to study point defects and grain boundaries in a number of metallic systems.

3. Results and discussion

3.1. Defect formation in CNT

In order to study the effect of interacting defects under thermo-mechanical loading, we consider (9.0) carbon nanotube with a length of 100 Å. A defect structure was generated by rotating two atomic bonds by 90° (Bonds 427–428 and 429–430 in Fig. 1). By this transformation, the hexagonal network of atoms is altered into a defected structure consisting of two 5-7-7-5 topological defects. When these defects are relaxed using molecular statics, they tend to reorient to a near sp^2 configuration. As a result of this, the ovality (defined as ratio of radius of the tube to radius of a perfect tube) of the CNT deviates from that of a perfect nanotubes. as shown in the Fig. 2a and b. In the following sections we present the observation based on simulation under pure mechanical loading, pure thermal loading and combined thermo-mechanical loading.

3.2. Effect of mechanical loading

For studying the effect of pure mechanical loading, tensile stresses were applied by displacing both the ends of nanotubes (15 Å on either side), followed by stabilization for 1500 time steps with a step size of 0.2 fs. The simulations are performed in isothermal conditions at a temperature of 77 K. In the present analysis, end displacements were applied incrementally until a strain level of 10% was reached. The atoms within the core of the defect were monitored during the simulation. These atoms undergo considerable radial displacement, such that the oval shape as observed initially (Fig. 2b) turns to a near circular configuration, as shown in Fig. 2c. Fig. 3 shows the variation of radial position of atoms 427 and 428 (forming the defect). It can be observed that the atoms move inward resulting in reduced ovality. Since the applied strain is in longitudinal direction, atoms are naturally displaced in the longitudinal direction. It is observed that there is no significant variation in bond length between the atoms 427 and 428.

It has been shown from molecular statics simulations [4] that when local stresses and strains were computed near the defected portion and a region away from the defect, stress and strain concentration effects occur near the defected region. Fig. 4 shows the variation of longitudinal stress along the length of the tube at different strain levels. In order to calculate the longitudinal stresses, the length of the CNT is divided into seven segments and in each segment, Lutsko stresses are computed over a region. Lutsko stress in the longitudinal direction is as shown in the Fig. 4. Stress concentration is observed near the defected region. Fig. 5 shows the atomic stresses (BDT stresses) for four atoms forming the core of the defect. Atoms 427 and 429 experience higher tensile stress than the inner atoms 428 and 430 of

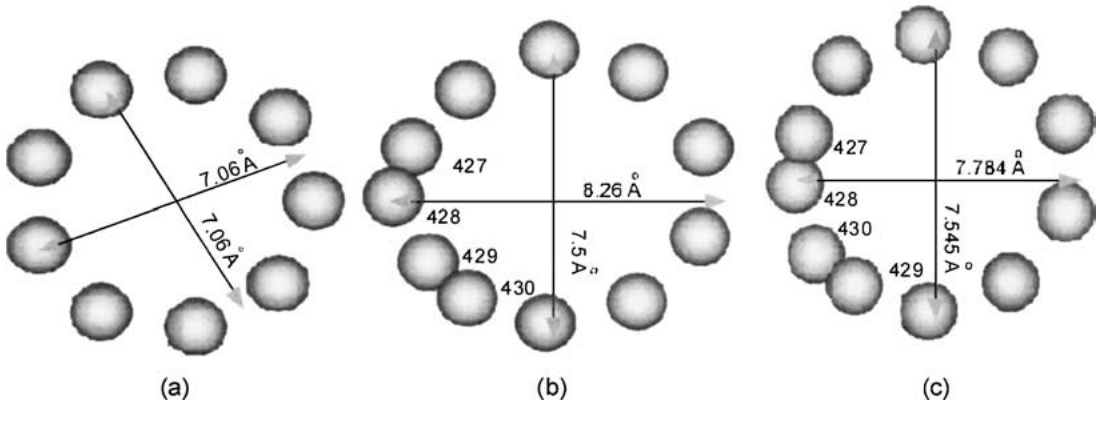

Figure 2 (a) A section of (9, 0) perfect tube showing atomic positions. (b) A section of defected portion of a (9, 0) tube showing atomic positions, and (c) A section of (9, 0) tube near defect when the tube is subjected to mechanical loading.

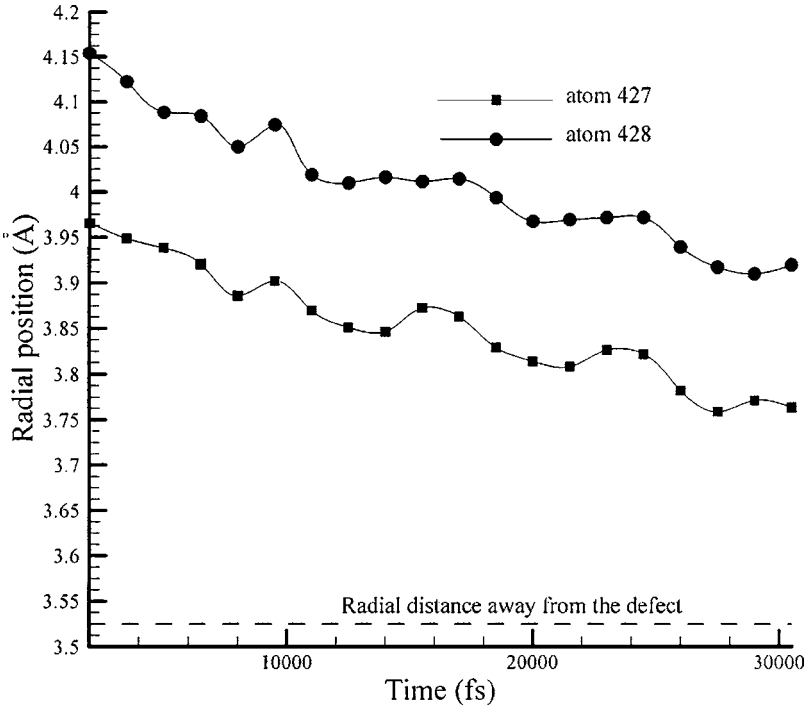

Figure 3 Variation of radial position of atoms 427–428 (upper defect) with mechanical loading.

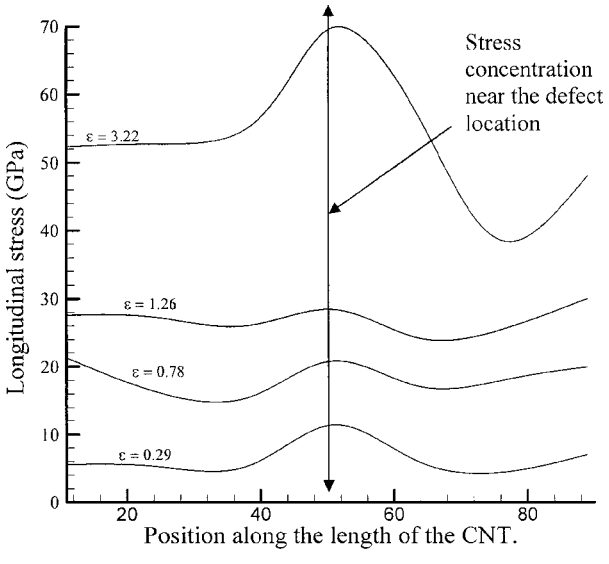

Figure 4 Variation of longitudinal stress along the length of the CNT under mechanical loading.

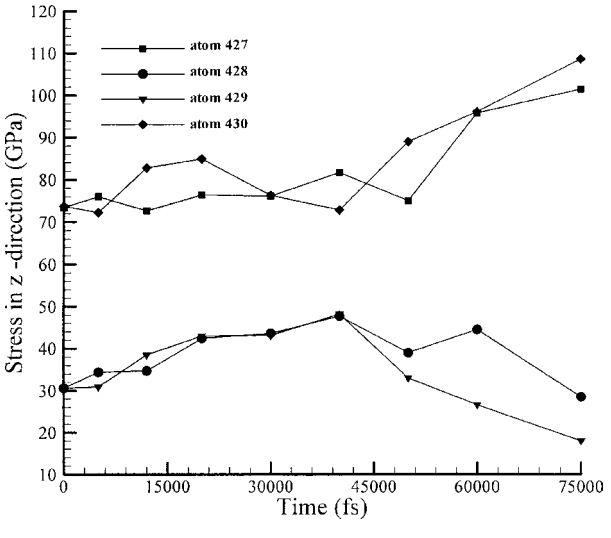

Figure 5 Variation of atomic (BDT) stress in *Z* direction (longitudinal stress) at few atomic locations near the defect due to mechanical loading.

the defect core. The atomic stresses vary monotonically without any random behavior. The defect structure did not change even at high strains. The mechanical loading provided considerable energy for each of the atom, but that is not enough to anneal the defects. This indicates that mechanical loading alone is not capable of the reconstruction process.

3.3. Effect of thermal loading

In order to study the effect of thermal loading on the CNT with topological defects as shown in Fig. 1, MD simulations were carried out on the tubes at different temperatures ranging from 300 to 3500 K. For the temperature range from 300 to 3000 K, the atoms exhibit thermal vibration in both radial and longitudinal directions about a mean position. Figs 6 and 7 show the atomic positions of atoms 427–428 in the radial direction and the longitudinal direction during thermal simulation. Fig. 6 also shows the variation in bond length between the atoms 427 and 428. Though the typical bond length of atoms in a perfect (with no defect) region is 1.44 Å, due to the effect of defect formation the bond length between atoms 427 and 428 is 1.39 Å, even before the application of any thermal (or mechanical) load. During thermal vibrations, the two atoms oscillate and when the distance between them is below the equilibrium distance, compressive separation forces are experienced which then pushes the atoms away from each other. When the motion takes the atoms farther away, then a state of tension exists which bring the

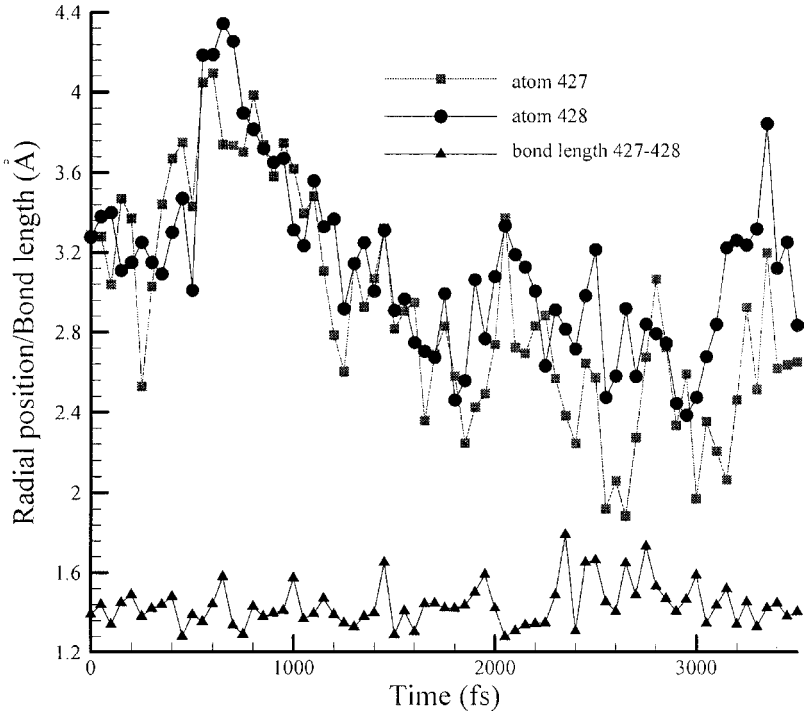

Figure 6 Variation of radial position and bond length of atoms 427–428 (upper defect) during thermal loading at 3000 K.

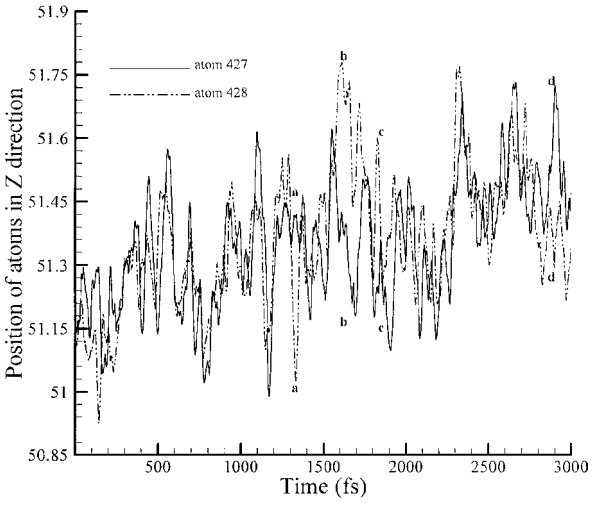

Figure 7 Variation of position of atoms 427–428 (upper defect) in Z direction during thermal loading ($T = 3000$ K).

atoms closer together. Such to and fro motion keeps repeating throughout the thermal loading as shown in Figs 6 and 7, without any change in defect structure. During thermal vibration the atoms forming the bonds (such as atoms 427–428) oscillate as one unit such that the pair of atoms either moves inwards or outwards in the radial direction. Similarly, the pair of atoms forming bond also oscillate in Z direction such that the pair either moves towards left or right. However at some instances as marked in the Fig. 7 as 'aa, bb, cc, and dd' the pair of atoms instead of moving together, they drift apart from each other. The adrift distance depends on the temperature of the system. Fig. 8 shows the variation of adrift distance with different temperature. During the thermal simulations at some instances (such as 'bb') the distance by which the two atoms move apart will be largest. Such larger distance of adrift for different temperature ranges is shown in Fig. 8. If at any instant the adrift distance reaches a value closer to that of bond length then such bond will rotate and stay in that configuration. The largest adrift distance is in the range of 0.5 to 0.6 Å, observed at a temperature range of 3000 K. At temperature range above 3000 K, the atoms disintegrate (melt), loosing its regular hexagonal pattern. Thus these simulations indicate that temperature increase alone is unable to bring about the reconstruction process.

3.4. Effect of thermo-mechanical loading

The above results from the two simulations (thermal and mechanical) show that the defect structure in the CNTs remain unaffected, when subjected to either mechanical loading or thermal loading independently. We next investigate the concurrent effect of thermal and mechanical loadings on the defect structure. Simulations were carried out on CNTs with defect as shown in the Fig. 1 by fixing one end of the tube (atoms over a length of 10 Å on left end are fixed in position) and applying tensile displacement to the other end (atoms over a end length 10 Å on right end are displaced), followed by stabilization for 1500 time steps with a step size of 0.2 fs. The temperature was maintained constant while the displacements were applied incrementally until a strain level of 5% is reached. Simulations were conducted for a temperature range of 77 to 2800 K, while mechanical loads were applied thus simulating the thermo-mechanical loading conditions. The defect structure did not change when the temperature was increased up to 2700 K. The change in defect structure was observed for temperature above 2800 K. At a temperature of 2800 K, when the applied strain level is approximately 2.3%, a change in defect structure is observed. It was mentioned earlier that the defect

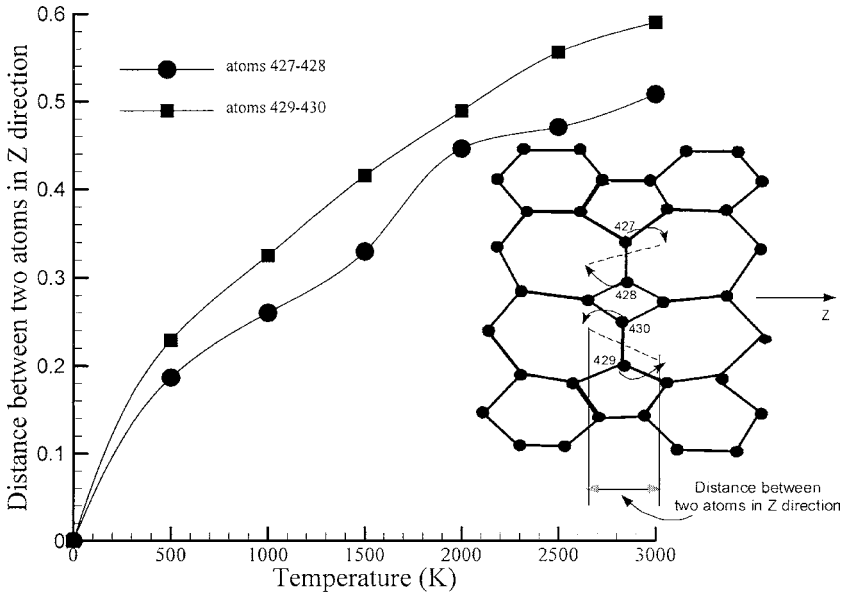

Figure 8 Variation of distance between atoms 427–428 (upper defect) and 429–430 (lower defect) in Z direction during thermal Loading. The inset depicts the process of thermal vibration.

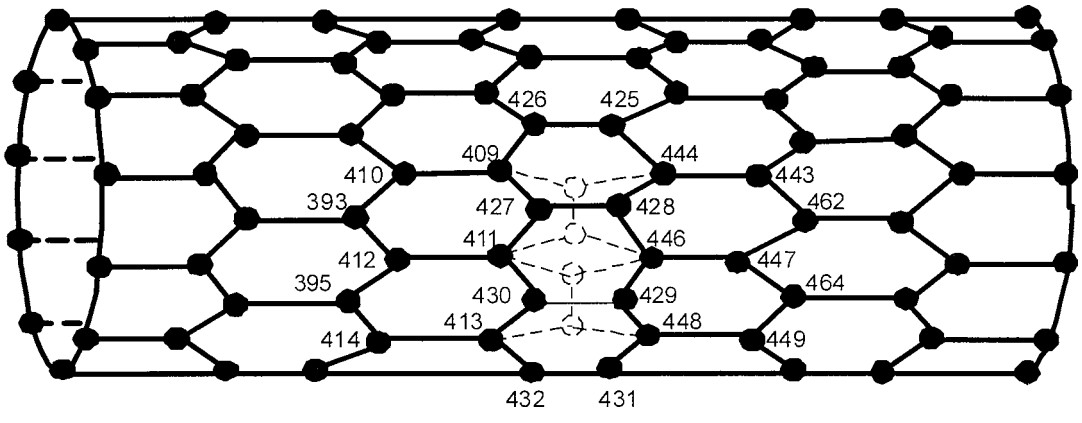

Figure 9 Annihilation of the two 5-7-7-5 defects placed along the circumference of the tube, under thermo-mechanical loading. The numbers indicate the atom numbers forming the defects.

structure was formed by rotating two horizontal bonds (427–428 and 429–430) CCW by 90°. When the CNT was subjected to the critical combination of thermo-mechanical loading, one of the bonds formed by the atoms 427–428 reverts back (CW) to its initial configuration, as shown in the Fig. 9. Upon further application of load, at a strain level of 4.26% and temperature of 2800 K, the lower defect also annihilated, when atoms 429 and 430 reverted to its initial configuration. Fig. 10 shows the sequence of atomic positions at different time intervals.

Fig. 11 shows the variation in the relative position of atoms 427 and 428 in the longitudinal. Z-direction during the thermo-mechanical loading. As observed during pure thermal loading, the two atoms move together either to the left or to the right as consequence of thermal vibrations. Initially the atoms remain together at same mean Z position of 51 Å. Because of thermal vibration, the two atoms oscillate about the mean position of 51 Å. Just before the bond reverts back to its initial configuration, the two atoms start drifting apart. When the adrift distance reaches a value of 1.44 Å (equilibrium distance between carbon atoms in a perfect tube is 1.44 Å) the bond rotates permanently and stays in that configuration. Fig. 11 shows that at approximately. 2.3% applied strain (approximately at 34500 fs) the two atoms move away in the opposite direction and subsequently remain in their position for the rest of the loading cycle. Similarly Fig. 12 shows the variation in the relative position of atoms 429 and 430 in the longitudinal, Z-direction during the thermo-mechanical loading. At around 4.26% applied strain (corresponding to 68000 fs) the two atoms start drifting apart and the distance of separation reaches a value of 1.44 Å, resulting in the annihilation of second defect.

During thermo-mechanical simulation, both Lutsko and atomic stresses were also monitored. The variation in atomic stresses in longitudinal direction for atoms 427 and 428 is shown in Fig. 13 and that of atoms 429 and 430 is shown in Fig. 14. There is a random variation of stresses in all the four atoms, unlike the situation observed in pure mechanical loading (Fig. 5). The randomness in the stress levels is due to thermal vibration experienced by all the atoms. When the bond 427–428 reverts back to its initial configuration, at that instant the stress level in atom 427 is tensile and in

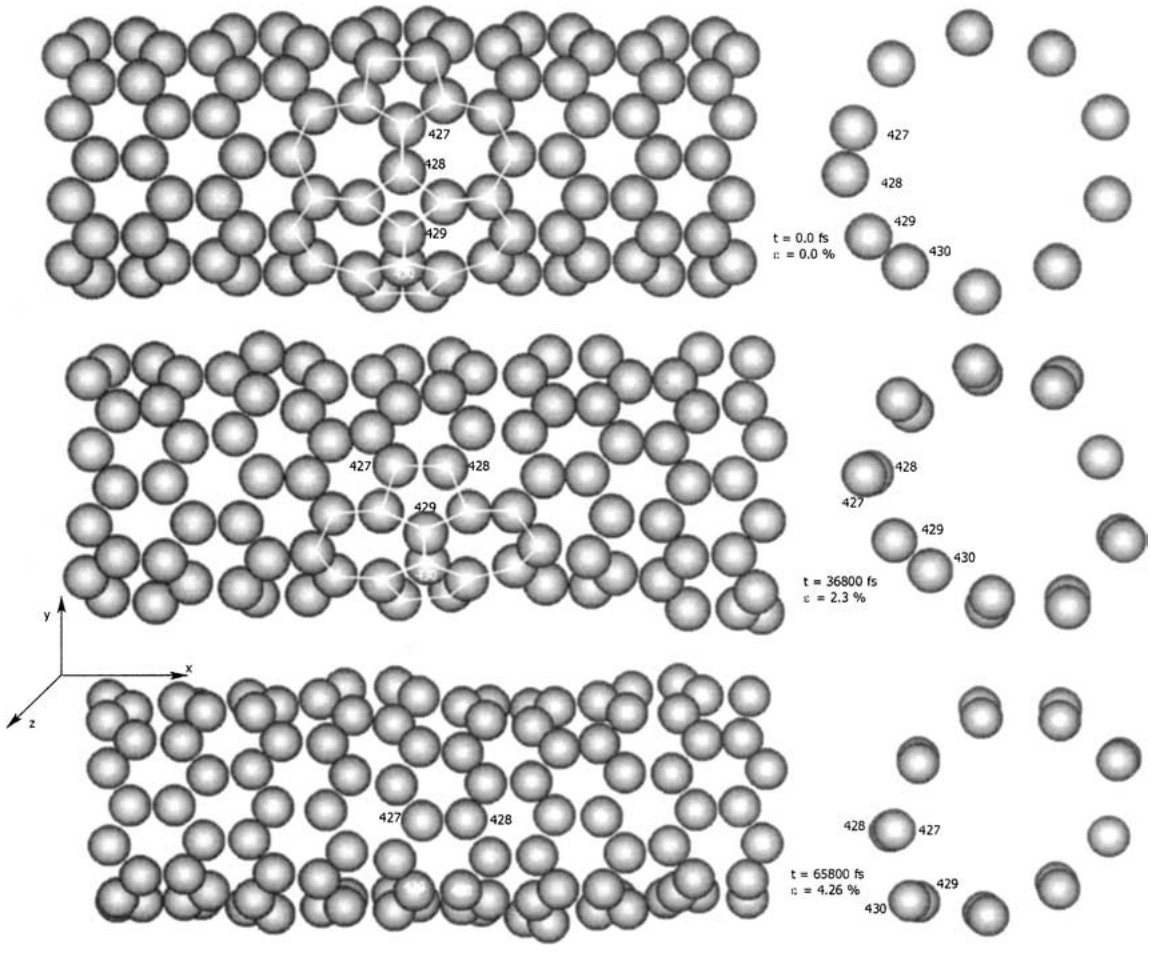

Figure 10 Sequence of annihilations process of two 5-7-7-5 defects at different time interval under thermo-mechanical loading.

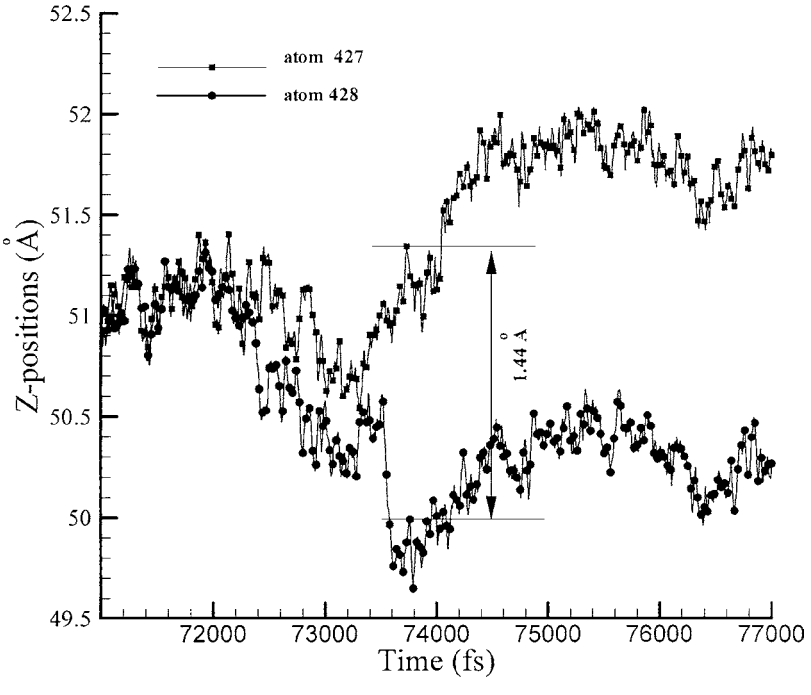

Figure 11 Variation of position of atoms 427–428 (upper defect) in the longitudinal (Z) direction during thermo-mechanical loading.

428 is compressive (Fig. 13), indicating that the forces experienced by the two atoms are in opposite directions. It can be recalled from Fig. 11 that during this period the atoms 427 and 428 are drifting apart. Just prior to the annihilation, atoms 429 and 430 experience a tensile force with stress levels of the order of 107 and 147 GPa respectively. At the instant of bond rotation, atom 429 suddenly is subjected to a compressive stress field due to which the stress reduces to the order of 39 GPa with a concomitant change of −68 GPa and

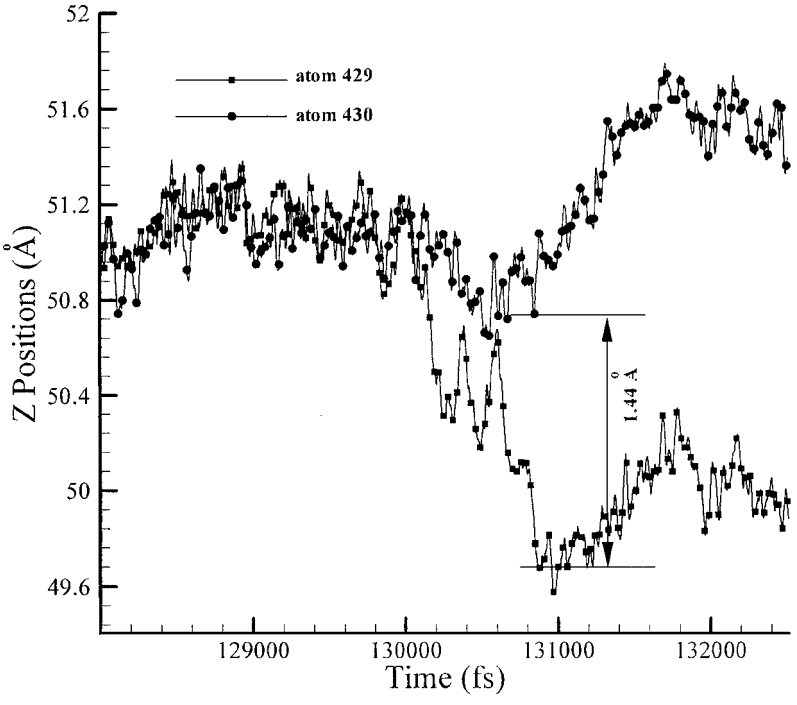

Figure 12 Variation of position of atoms 429–430 (upper defect) in the longitudinal (Z) direction during thermo-mechanical loading.

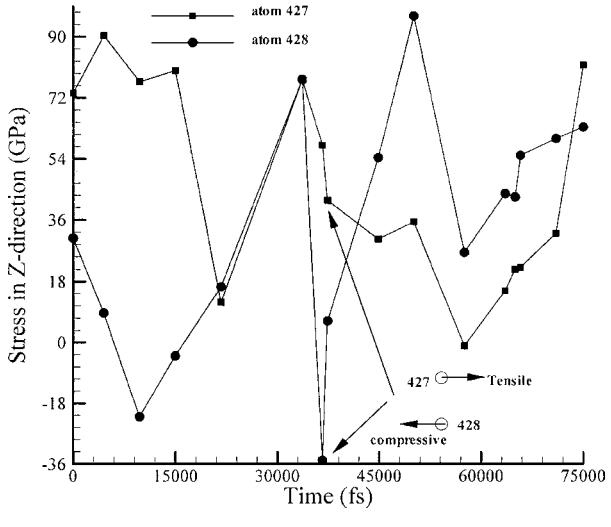

Figure 13 Variation of atomic stress in Z-direction (longitudinal stress) for atoms 427–428 of upper defect.

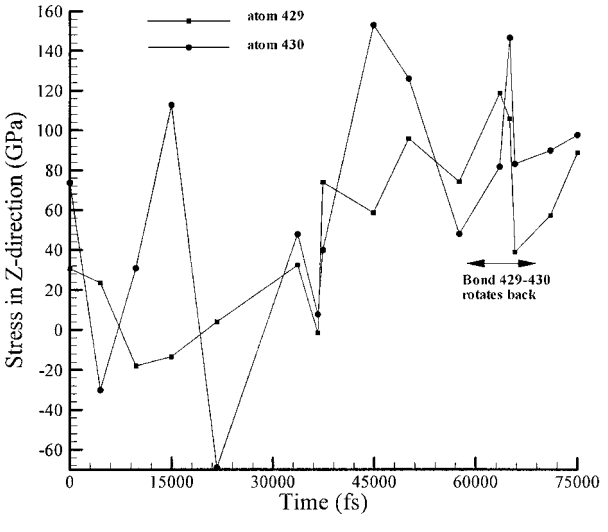

Figure 14 Variation of atomic stress in Z-direction (longitudinal stress) for atoms 429–430 (lower defect).

such a sudden change causes the drifting of the atoms as shown in Fig. 12 and is responsible for the bond to rotate.

3.5. Energy barrier

In the earlier discussion it has been shown that the combined effect of thermal vibration and tensile loading causes a bond in the core of the defect to rotate by 90°. In this section, we present results on the energetics of atoms forming the core of the defect. We note that there are two sets of defects, with atoms 428 and 427 forming the upper 5-7-7-5 defect while atoms 429 and 430 form the lower 5-7-7-5 defect. The atoms in the core of the defect will have higher energy configuration, which is energetically unstable and these atoms try to reach a stable configuration. To study the energy variation during this process, we monitored the total potential of atoms forming the core of the defect (427–428 and 429–430) during the entire thermo-mechanical loading. Fig. 15 shows the total potential energy variation of atoms 427 to 430. The mean potential energy per atom for a stable configuration is approximately −6.8 eV. It can be noted that atom 428 of the upper defect and atom 429 of the lower defect are in stable energetic condition even before the bond rotation (energy for these atoms are lower than −6.8 eV). On the other hand, atoms 427 of the upper defect, and atom 430 from the lower defect possess higher (unstable) energy (−6.0 eV) before the bond rotation takes place. This indicates that both the bonds (427–428 and 429–430) have equal chances of reverting to its initial configuration of a perfect CNT. In order for the bonds to rotate back to its initial configuration, two of the four atoms

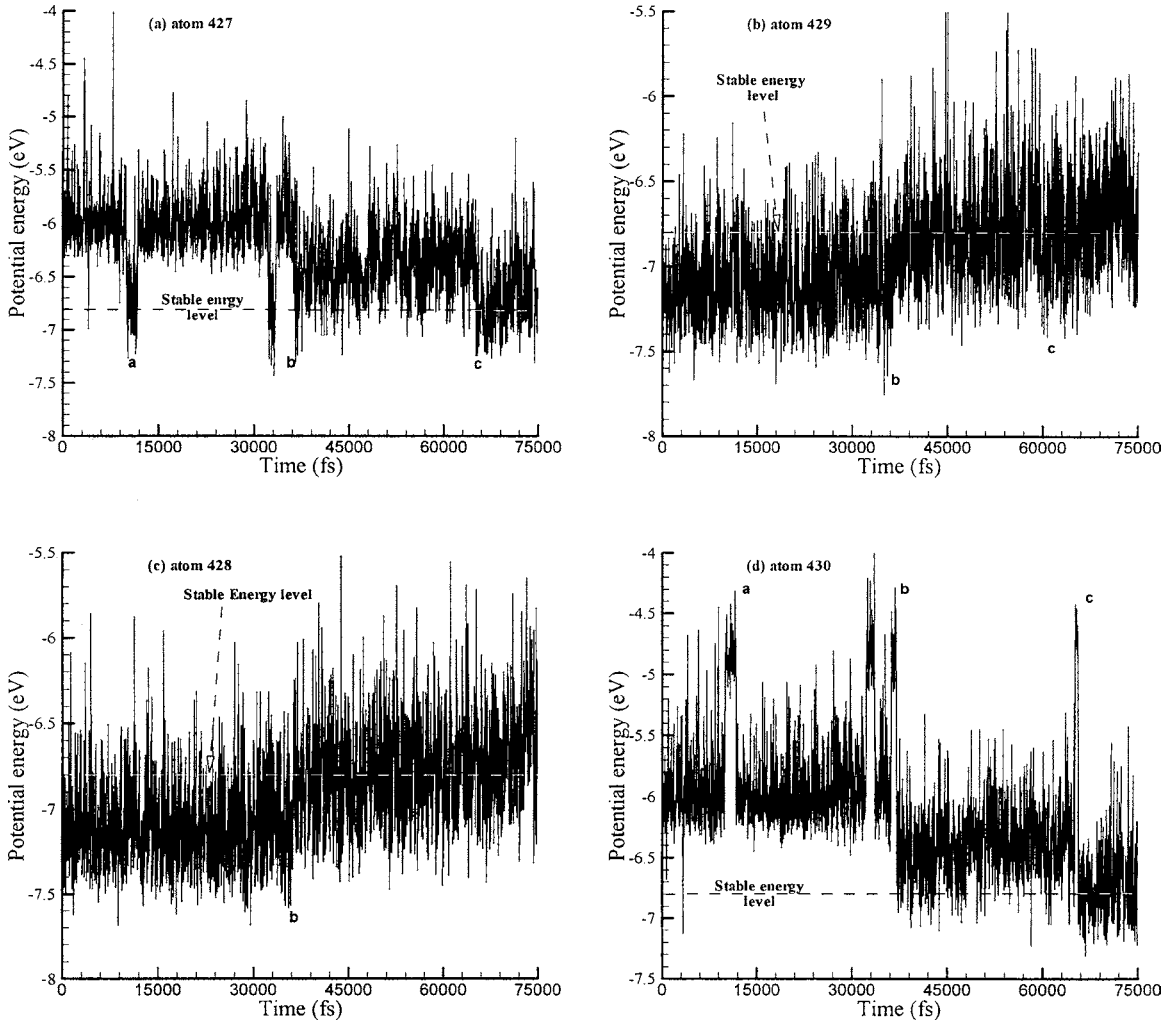

Figure 15 Variation of potential energy of atoms 427–428 of the upper and atoms 429–430 of the lower defects during thermo-mechanical loading.

(427 and 430) should overcome the barrier energy. The barrier energy depends on chirality and diameter of the CNT and it reduces with mechanical loading. From the Fig. 15a and d it can be observed that at 9500 fs, the atoms 427 and 430 make the first albeit an unsuccessful attempt to cross the energy barrier of 2.0 eV indicated by letter 'a'. At this instant the bonds do not rotate and hence they still in remain in unstable energy state. Again at 36000 fs, the atoms 427 and 428 once again crosses the energy barrier of 2.0 eV indicated by letter 'b' and this time the bond (427–428 of upper defect) rotates back to its initial configuration and also energy level of the atoms also reaches a quasi stable energy state (atoms 427 and 430 is at −6.5 eV, 428 and 429 nearer to −6.8 eV). Finally at 68000 fs, atom 430 once again crosses the energy barrier indicated by letter 'c', in Fig. 15d at which instant the bond 429–430 rotates back to stable configuration. After these events all the four atoms attain a stable energy level of −6.8 eV. By this process a CNT with defect turn to a perfect tube without any defect.

3.6. Process of defect annihilation

From the above discussion we observe that mechanical loading or thermal loading acting alone would not cause defects to annihilate, whereas a combination of thermo-mechanical loading brings about the annihilation. We

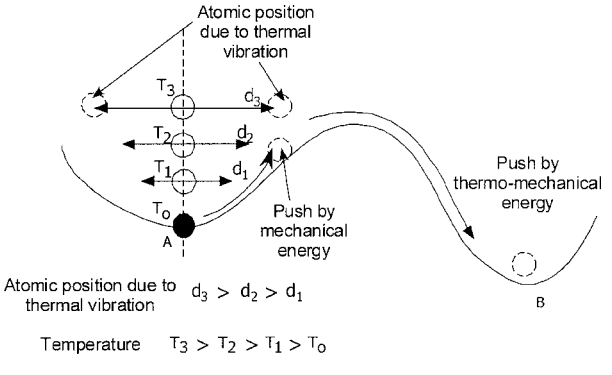

Figure 16 Schematic of atomic jump across the energy barrier from a unstable energy configuration A to stable configuration B under the combined effect of thermo-mechanical loading.

attempt to explain this phenomenon using heuristic arguments through a schematic in Fig. 16. As explained in the previous section (Fig. 15), the atoms 427 and 430 are unstable with a energy of −6.0 eV (the stable energy being −6.8 eV). Fig. 16 shows two local energy minima states at A and B with an energy barrier in-between. Our results indicate that this energy barrier is of the order 2 to 2.5 eV. We can presume that atoms 427 and 430 are at unstable minima state A. If these two atoms were to reach a stable configuration B, then these two atoms have to overcome the energy barrier.

Application of only thermal loading (Figs 6 and 7) induces atomic vibration to all atoms. While the atoms as a set (atoms 427 and 428) tend to vibrate in tandem (Fig. 7), they drift apart some times. This adrift distance increases with the system temperature as seen in Fig. 8. Schematic shows that the amplitude of oscillation increases with temperature, thus the amplitude d_3 at T_3 is larger than d_2 at T_2 and larger than d_1 at T_1. The adrift distance has to be 1.44 Å for permanently crossing the barrier. Our results indicate that the maximum adrift distance is 0.6 Å, indicating that thermal loading alone would not cause the atoms to cross energy barrier. Application of pure mechanical loading increases the distance of separation as shown (Fig. 16) by the movement of atom along the curved path. All the atoms experience forces of interaction, which will be predominantly in Z direction inducing longitudinal stress in the CNT (Figs 4 and 5). There is no significant increase in adrift distance between the two atoms as observed in thermal simulation. As discussed earlier, mechanical loading alone cannot cause defects to overcome the energy barrier even after applying 10% strain to the CNT. However when a critical combination of thermo-mechanical loading was applied to the system, the required synergy is achieved. When the temperature of the system is around 2800 K, thermal vibration in the atoms causes the two atoms forming the defect drift apart considerably, and at the same time there will be differential forces acting in Z direction on the atoms forming the core of the defect. This combined effect is sufficient to trigger the atoms forming the core of defect to jump over the energy barrier and reach a lower energy configuration indicated by 'B' in the Fig. 13. Once the unstable atoms cross over the energy barrier, the bonds forming the core of the defect rotate back to its original configuration, which results in lowering energy level of atoms associated with the defects.

4. Summary

Topological defects formed either during manufacturing or during thermo-mechanical loading can disappear under specific combination of concurrent thermal and mechanical loading conditions. However, our simulation results show that the application of either the thermal or the mechanical loading independently may not be able to achieve this defect annihilation. For example two adjacent Stone-Wales (5-7-7-5) defects in a (9,0) carbon nanotube can remain stable when thermal loading ranging from room temperature all the way to melting temperature is applied. Similarly when the tube is subjected to pure tensile strains up to 10% (at low temperatures when thermal effects are negligible) the same defects can remain stable. On the other hand, both the defects annihilate when the system is maintained at a temperature of 2800 K and then subjected to a tensile strain of 5%. In fact the first defect annihilates at a lower strain of 2.3%. Energetic analysis show that while the temperature promotes increased vibration about a mean position, the mechanical loading provides the sufficient and necessary displacement push for the defects to annihilate.

Acknowledgments

The authors wish to acknowledge the research collaborations with Professors Leon van Dommelen and Ashok Srinivasan during various phases of this work as a part of the Computational nanotechnology group at Florida State University. The funding provided by U.S. Army (Project monitor: Dr. Bruce La Mattina) is also gratefully acknowledged.

References

1. IIJIMA, *Nature* **354** (1991) 56.
2. T. W. EBBESEN and T. TAKADA, *Carbon* **33**(7) (1995) 973.
3. V. H. CRESPI, M. L. COHEN and A. RUBIO, *Phys. Rev. Lett*. **79**(11) (1997) 2093.
4. N. CHANDRA, S. NAMILAE and C. SHET, *Phys. Rev.* B **69** (2004) 094101.
5. T. KOSTYRKO, M. BARTKOWAIK and G. D. MAHAN, *ibid*. **59**(4) (1999) 3241.
6. J. C. CHARLIER, T. W. EBBESEN and P. LAMBIN, *ibid.* **53** (1996) 11108.
7. Z. YAO, H. W. C. POSTMA, L. BALENTS and C. DEKKER, *Nature* **402**(6759) (1999) 273.
8. M. B. NARDELLI, B. I. YAKOBSON and J. BERNHOLC, *Phys. Rev*. B **57** (1998) 427.
9. M. B. NARDELLI and B. I. YAKOBSON, *Rev. Lett*. **81**(21) (1998) 4656.
10. B. I. YAKOBSON, C. J. BRABEC and J. BERNHOLC, *Phys. Rev. Lett*. **76**(14) (1996) 2511.
11. M. B. NARDELLI, J. L. FATTEBERT, D. ORLIKOWSKI, C. ROLAND, Q. ZHAO and J. BERNHOLC, *Carbon* **38** (2000) 1703.
12. L. G. ZHOU and S. Q. SHI, *Comp. Mater. Sci.* **23** (2002) 166.
13. E. KAXIRAS and K. C. PANDEY, *Phys. Rev. Lett*. **61** (1988) 2693.
14. B. C. PAN, W. S. YANG and J. YANG, *Phys. Rev*. B **62** (2000) 12652.
15. P. ZHANG, P. E. LAMMERT and V. H. CRESPI, *Phys. Rev. Lett*. **81** (1998) 5346.
16. P. M. AJAYAN, V. RAVIKUMAR and J. C. CHARLIER, *ibid*. **81** (1998) 1437.
17. M. KOSAKA, T. W. EBBESEN, H. HIURA and K. TANIGAKI, *Chem. Phys. Lett*. **233** (1995) 47.
18. Y. WANG, W. HUANG, F. WEI, G. H. LUO, H. YU and T. J. AIHEMAI, *Chem. J. Chin. Univ*. **24**(6) (2003) 953.
19. C. SHET, N. CHANDRA and S. NAMILAE, *Mech. Adv. Mater. Struct.* (2004) (accepted).
20. J. F. LUTSKO, *J. Appl. Phys*. **64** (1988) 1152.
21. J. CORMIER, J. M. RICKMAN and T. J. DELPH, *ibid.* **89** (2001) 99.
22. Z. S. BASINSKI, M. S. DUESBERRY and R. TAYLOR, *Canadian J. Phys*. **49** (1971) 2160.

Received 9 February
and accepted 24 May 2004